

Vortex generation in electroosmotic flow passing through sharp corners

Jia-Kun Chen · Ruey-Jen Yang

Received: 8 April 2008 / Accepted: 19 May 2008 / Published online: 31 May 2008
© Springer-Verlag 2008

Abstract A special phenomenon was found when sharp wedges were set in a microchannel where electroosmotic flow occurred, vortices were induced near the wedges when a DC electric field was imposed. The strength of the induced vortices depends on the concentration of electrolytes and the intensity of the electric field. Latex particles are used to aid the flow visualization. Formation of vortices is due to concentration depletion in the microchannel. Furthermore, the vortices are used to enhance mixing in a micromixer. Experimental results showed that the vortex structures created within the mixing section increase the mixing index from a value of 3% in the upstream region of the microchannel to 78% at the outlet of the mixing section.

Keywords Concentration depletion · Vortex · Microfluidics · Micromixing

1 Introduction

Microfluidic devices, lab-on-a-chip systems, and micro total analysis systems (micro-TAS) applications have attracted considerable attention over the past decade as a means of performing a variety of bioanalytical and chemical processing tasks. Electroosmotic flow (EOF) has emerged as the method of choice for manipulating fluids in such microdevices, and many applications of EOF have been presented in the literature (Johnson and Locascio

2002; Lazar and Karger 2002; Glasgow et al. 2004; Lin et al. 2004; Hardt et al. 2005; Wu et al. 2005; 2007, etc.).

In practical microfluidic applications, it is frequently necessary to achieve a thorough mixing of two or more species (Chang and Yang 2007). The characteristic velocity of EOF is generally described by the Smoluchowski equation, i.e. $\bar{V}_{\text{slip}} = \frac{\varepsilon\varepsilon_0\zeta}{\mu} \nabla\phi$, where ε is the dielectric permittivity of the solvent, ε_0 is the permittivity of a vacuum, ζ is the zeta potential, μ is the viscosity of the fluid and $\nabla\phi$ is the external potential gradient (Probstein 1994). The Smoluchowski equation indicates that the characteristic velocity varies linearly with the magnitudes of the zeta potential and the external potential drop. The related flow phenomena are generally referred to as classical linear EOF and are characterized by a Reynolds number of less than 1. Cummings et al. (2000) demonstrated the similitude between the flow streamlines and the electric field lines in linear EOF given a neutral fluid with a uniform density, viscosity, and conductivity and a uniform surface zeta potential at the fluid–solid interface. In other words, the characteristics of the linear EOF are similar to those of inviscid potential flow, which is irrotational. The generation of vortices in linear microfluidic systems is difficult. In such systems, the species flow tends to be laminar, so species mixing takes place primarily as a result of molecular diffusion. Molecular diffusion, however, is an inherently slow process, so achieving an adequate species mixing performance requires the use of a long mixing channel and a long retention time. To improve the mixing efficiency of microfluidic devices, researchers have paid increasing attention to the feasibility of utilizing nonlinear electrokinetic phenomena to agitate the species streams within the microchannel. Bazant's group (Bazant and Squires 2004; Squires and Bazant 2004) studied the “nonlinear electrokinetics” generated when a conductor is

J.-K. Chen · R.-J. Yang (✉)
Department of Engineering Science,
National Cheng Kung University, Tainan, Taiwan, ROC
e-mail: rjyang@mail.ncku.edu.tw

placed within an AC or DC electric field. Bazant et al. (2004) investigated the boundary conditions required to induce the nonlinear electrokinetic effect near electrode surfaces. Olesen et al. (2006) focused on the effect of geometrical confinement, Faradaic current injection, and the nonlinear surface capacitance of AC nonlinear electrokinetic micropumps.

In this study, we found that the vortices could be induced when a wedge was set into a channel without any AC EOF systems. Generally, the vortices are not easily induced in a low Reynolds number flow even when the flow passes around a sharp wedge. Vortices are rare in DC microfluidic systems especially in DC EOF (electrokinetic instability was not discussed here). Recently, Levitan et al. (2005) used a similar geometry showing induced-charge electro-osmosis (ICEO) with AC fields in microfluidics. They set a metal wire in the microchannel and vortices were induced near the metal wire. Thamida and Chang (2002) and Yossifon et al. (2006) reported that vortices are formed near the corners of microchannel intersections in microfluidic devices once the magnitude of the externally applied DC electric field exceeds a certain threshold value. Large field penetration exists near a corner of the channels. The external field can penetrate the double layers and produce non-equilibrium electrokinetics near sharp corners. The fabrication of a sharp corner (the radius of the curvature is around 10 nm) needs a very precise manufacturing process. Our facilities can at best fabricate sharp corners with a radius around 10 μm , which means that electric field penetration was not the major reason for the vortices induced near the wedge in our study.

Utilizing Ohm's law to determine the current density near the corner, the similitude between the electric field lines and streamlines that described by Cummings et al. (2000) is realized. In other words, vortices should not be formed near the corner features, but the experimental observations presented later in this study reveal that vortex structures were, in fact, formed near the corners in the microchannel. Recently, Park et al. (2006) demonstrated that vortices could be formed in a bottleneck of a constricted channel under DC EOF. They explained it in terms of finite double layer thickness effects. Chu and Bazant (2006) gave a theory for nonlinear relaxation effects with thin double layers around conducting protrusions from a channel wall. They predicted concentration gradients due to salt adsorption and surface conduction in the double layer near the edges. Takhistov et al. (2003) argued that the vortex structures could be attributed to a local concentration depletion effect prompted by the requirement to maintain a balance of the electrical current near the corner in the microchannel. The authors showed that the concentration depletion effect led to an increased zeta potential at the corner and therefore increased the EOF slip velocity

at the walls. This phenomenon is generally referred to as "DC nonlinear electrokinetics". Because of the concentration depletion near the sharp wedge, the zeta potential is altered according to the concentration distribution. The above mechanism should be the major cause of vortex formation near a sharp wedge presented in this study. A similar topic was studied by Bazant et al. (2007). They demonstrated that by varying the salt concentration can affect the electroosmotic flow velocity.

In this paper, we investigated the above-mentioned flow physics near the sharp wedge in the microchannel. Furthermore, we applied this phenomenon to enhance micromixing for a micromixer. Accordingly, the current study presents a novel micromixer composed of a serrated mixing channel in which a DC nonlinear electrokinetic effect is used to enhance species mixing. The experimental results reveal that, when two species streams were introduced simultaneously into the microchannel, the vortices induced by the concentration depletion effect near the individual serrations in the mixing section constrained both streams to flow through the central region of the microchannel. As a result, the mixing distance between them was significantly reduced, thus achieving an improved species mixing effect.

2 Materials and methods

Figure 1 illustrates the basic geometry of the microchannel employed to examine the effect of a single pair of wedges (referred to henceforth as "corners") on the flow structures generated within the fluid stream. As shown, the inlet and outlet reservoirs had a diameter of 4 mm, while the mixing channel had a length, width and depth of 1 cm, 200 and 45 μm

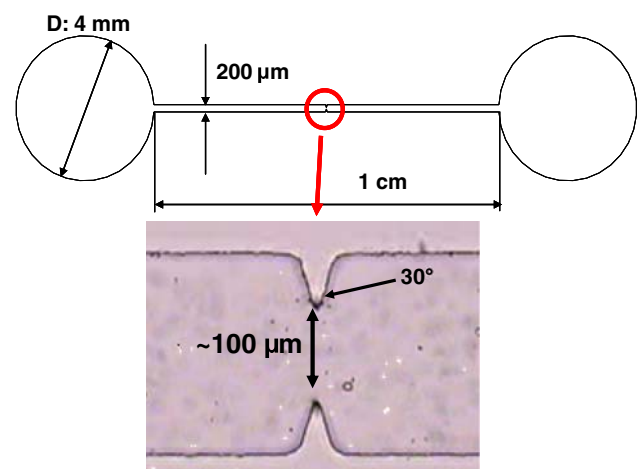


Fig. 1 Microchannel depth is 45 μm ; width is 200 μm ; length is 1 cm; reservoir diameter is 4 mm. The corners have an apex angle of 30° and are separated by a distance of approximately 100 μm

μm , respectively. The individual corners had an apex angle of 30° and were separated by a distance of approximately $100\ \mu\text{m}$. The microchannel was fabricated from polydimethylsiloxane (PDMS). In the fabrication process, silicone elastomer and elastomer curing agent (Sil-More Industrial Ltd, USA Sylgard 184A and Sylgard 184B) were mixed in a ratio of 10:1 and then poured onto an SU-8 mold. The PDMS was cured at a temperature of 70°C for one hour and then treated using oxygen plasma to change its inherent hydrophobic surface property to a hydrophilic property. The PDMS inverse structure was then peeled off the template and bonded with a flat glass substrate. Full details of the fabrication process are presented in McDonald and Whitesides (2002).

To observe the flow fields induced within the microchannel under the application of an external DC electric field, latex particles with a diameter of $3\ \mu\text{m}$ were introduced into the sample. Having examined the flow structures induced by the DC nonlinear electrokinetic effects, a series of mixing experiments was performed using Rhodamine B as the sample and de-ionized water as the electrolyte. During these experiments, the flow structures were observed using a mercury lamp induced fluorescence technique. The experimental images were captured by an optical microscope (Model: Eclipse 50i, Nikon, Japan), filtered spectrally, and then observed using a charge-coupled device camera (CCD, model: SSC-DC50A, Sony, Japan). The mixing effectiveness within the microchannel was quantified based on the intensity of the Rhodamine B sample using the mixing index presented in Lin et al. (2005) and Chen and Yang (2007), i.e.

$$M = \left(1 - \frac{\int_A |c_i - c_\infty| dA}{\int_A |c_0 - c_\infty| dA} \right) \times 100\% \quad (1)$$

where c_i is the concentration distribution at the outlet of the serrated mixing section, c_0 is the concentration at the inlet of the serrated mixing section, and c_∞ is the concentration of complete mixing.

3 Results and discussion

In Fig. 2, the intensity of the electric field was $500\ \text{V/cm}$, and three electrolytes were used. The strength of the induced vortex increased when the concentration of the electrolytes decreased. The decreased concentration resulted in a thicker electrical double layer (EDL). Furthermore, the thicker EDL induced a higher zeta potential. The concentration depletion near the sharp wedge had a more pronounced effect when the electrolyte had a more dilute concentration. The red dash line marks the region of the induced vortices in Fig. 2. In Fig. 3, the channel was filled with DI water, and the three different intensities of the

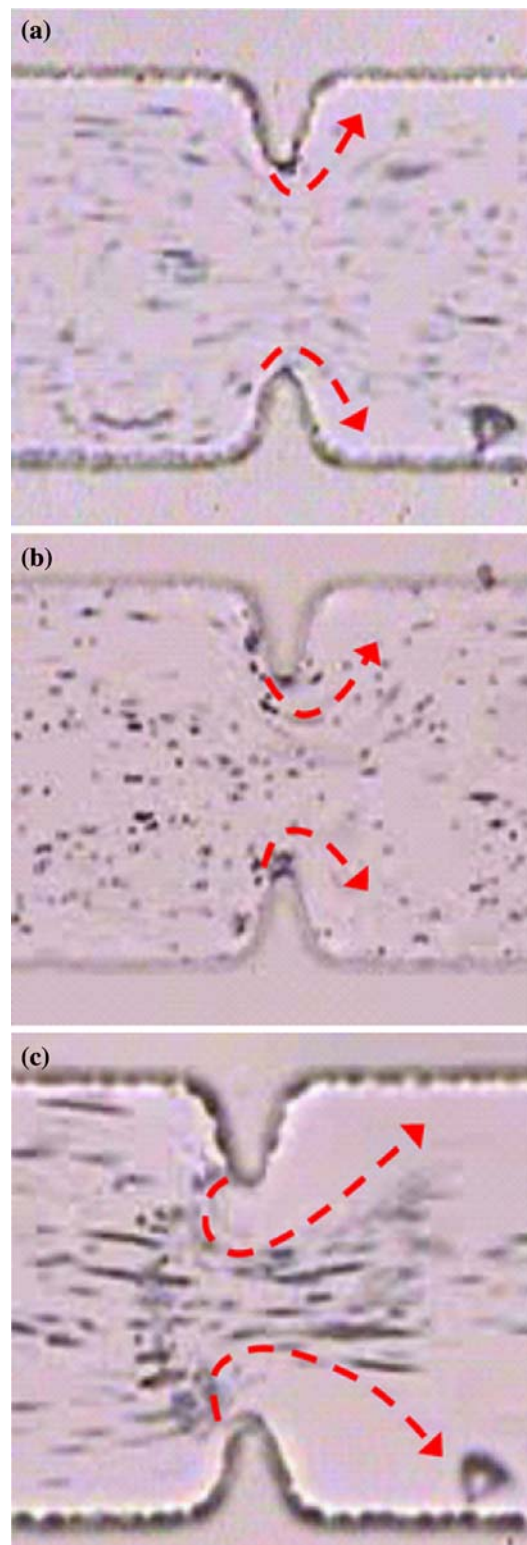


Fig. 2 The intensity of the electric field was $500\ \text{V/cm}$. **a** NaCl $10\ \text{mM}$; **b** NaCl $1\ \text{mM}$; **c** DI water

electric field were imposed on the system. The strength of the induced vortex trends with the intensity of the electric field. The vortices in the Figs. 2 and 3 were greatest in DI

water and then decreased with increasing the concentration of the electrolyte. This observation is consistent with all other experiments on related induced-charge electrokinetic phenomena (Studer et al. 2004; Urbanski et al. 2006; Bazant et al. 2007; Gangwal et al. 2008).

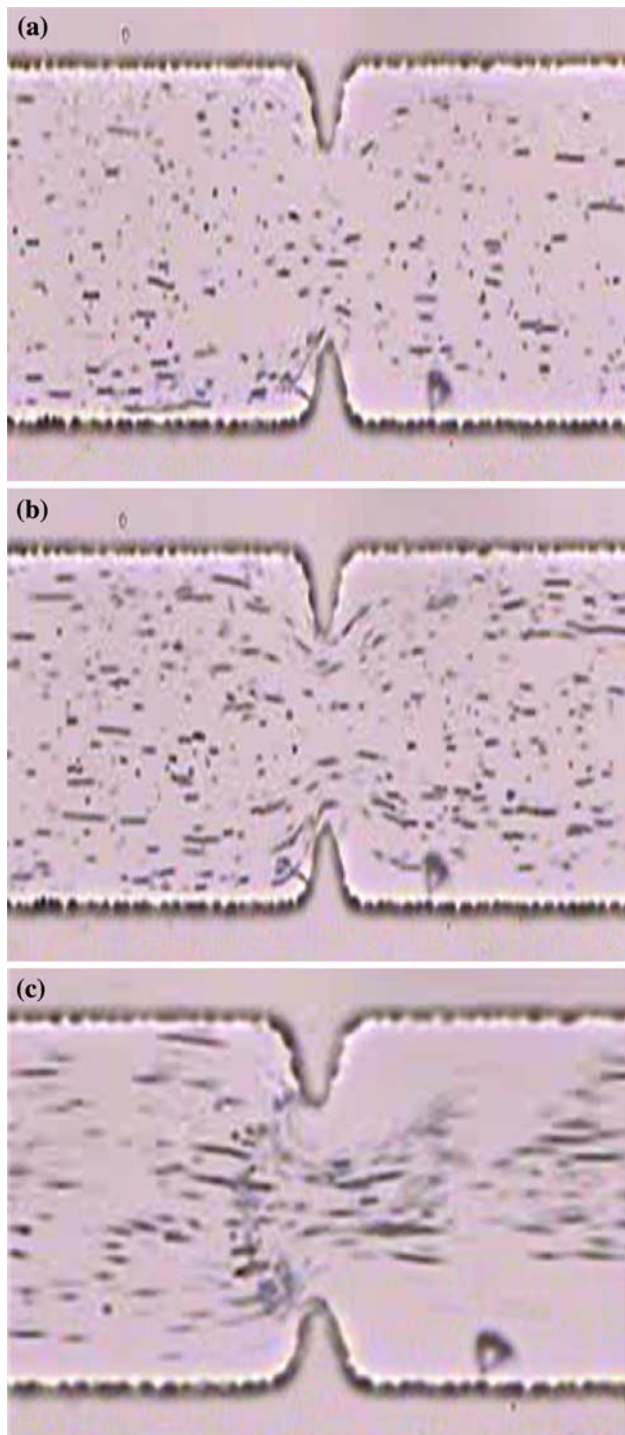


Fig. 3 The channel was filled with DI water. **a** 150 V/cm; **b** 200 V/cm; **c** 500 V/cm

Figure 4a illustrates the flow structures induced within the microchannel by an external DC electric field with an intensity of 500 V/cm. It was observed that some latex particles aggregated in the upstream region of the flow near the tips of the two corners. This suggests the formation of closed vortex structures within the fluid stream. These vortices formed a nozzle-like structure between the two symmetrically-opposed corners, as indicated by the dashed lines in the figure. The nozzle compressed the fluid stream and accelerated it along the center of the microchannel. Therefore, the flow structures induced in the microchannel were influenced by the EOF effects imposed by the side-walls. As discussed above, however, the fluid in the central region of the channel forms vortex structures as a result of a concentration depletion effect near the corners. Figure 4b

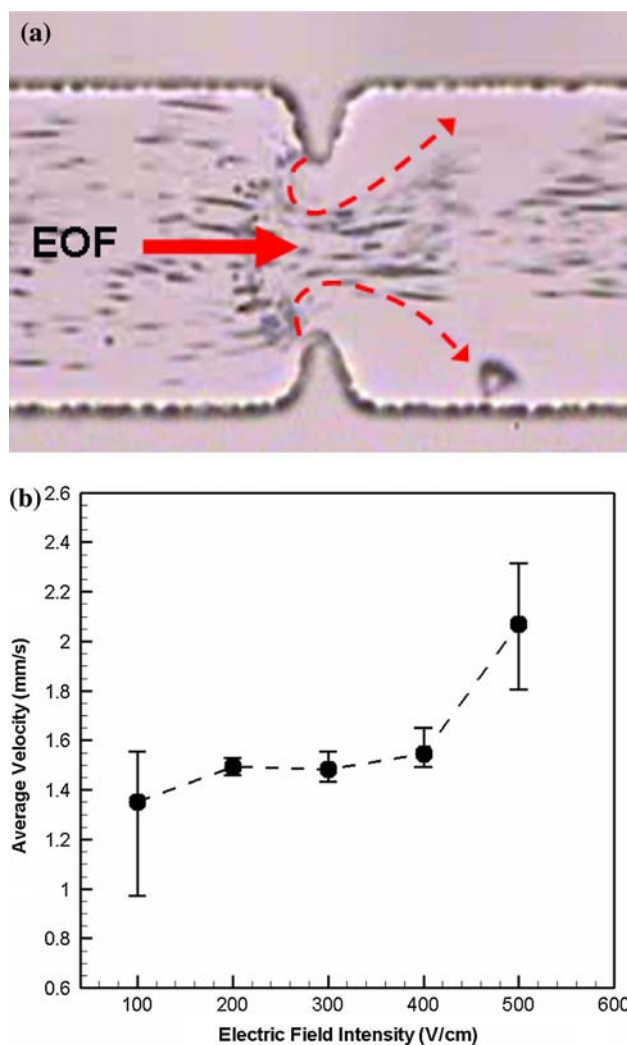


Fig. 4 a Vortices formed near corners when DC electric field of intensity 500 V/cm is applied. The vortex regions are marked using red dashed lines for clarity. **b** Relationship between the average velocity of particles flowing between the corners and the intensity of the external DC electric field

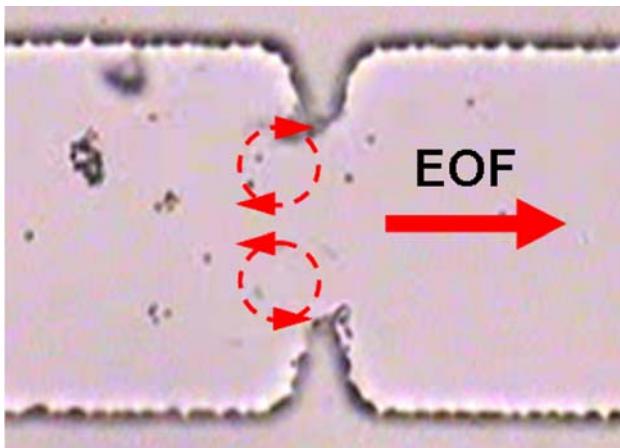


Fig. 5 DC electric field of 500 V/cm is applied resulting in the formation of vortices (as indicated by red dashed lines). The velocity of trapped particle was around 6.59 mm/s

illustrates the relationship between the average velocity of the particles near the corners and the intensity of the external DC electric field. Note that the velocity data are related to the latex particles traveling in the streamwise direction of the flow field rather than those circulating within the vortex structures. It is observed that the average velocity remained constant at approximately 1.5 mm/s as the intensity of the electric field increased from 100 to 400 V/cm, but average velocity increased sharply to 2.07 mm/s when the electric field was increased to 500 V/cm. This increase is due to the induced vortex, which had a nozzle-like effect along the flow passage.

Figure 5 illustrates the formation of vortex structures upstream of the corners under a DC electric field with an intensity of $E \sim 500$ V/cm. As shown, the lower vortex rotated in a counter-clockwise direction, while the upper vortex rotated in a clockwise direction. The zeta potential on the walls of the current PDMS microchannel containing de-ionized water was estimated to be of the order of 30 ~ 40 mV, and the velocity of classical EOF was around 1.06 mm/s under an electric field of an equivalent intensity. In contrast, the experiments indicate that the velocity near the corner was estimated to be 6.59 mm/s. The relatively higher velocity of the flow near the corner region of the channel compared to that in other regions of the channel produced a back pressure, which prompted the formation of the vortex structures in the upstream region of the corners. It has been reported that sharp corners in a microchannel

induce a concentration depletion effect in the electrolyte, which in turn changes the zeta potential on the microchannel surface (Takhistov et al. 2003; Bazant et al. 2007). The higher velocity observed near the corner regions of the current microchannel suggests that the zeta potential increased in the corner regions. It is observed that the directions of rotation of these two vortices are equivalent to those observed experimentally in Fig. 5. According to Probstein (1994), the zeta potential on the microchannel wall, ζ , is related to the electrolyte concentration, c , as follows:

$$\zeta \sim c^{-1/2}. \tag{2}$$

The two vortices forced the fluid stream to flow along the central region of the microchannel. Thus, if two sample fluids were introduced simultaneously into the channel, the mixing distance between them would be reduced, thus enhancing the mixing index (Chen and Yang 2007). Table 1 summarizes the mixing indices computed using Eq. (1) in regions of the microchannel immediately upstream and downstream of the corners under various values of the external DC electric field. In general, the relative contributions of dispersion and diffusion to the advection effect within the microchannel can be quantified via the Peclet number, given by

$$Pe = \frac{UL}{D}, \tag{3}$$

where U is the characteristic fluid velocity within the channel, L is the characteristic length of the channel, and D is the diffusion coefficient of the electrolyte. As the intensity of the electric field is increased, the velocity of the electrolyte also increases, and thus a higher value of the Pe number is obtained. A higher Pe number indicates that the flow field within the microchannel is dominated by the effects of convection rather than diffusion. As a result, the mixing indices that are shown in Table 1 decrease as the value of the external DC electric field is increased. Nonetheless, it is clear that, for a constant value of the DC electric field, the mixing index is significantly improved by the presence of the corners.

Having verified the effectiveness of a single corner pair in enhancing the mixing index within the microchannel, a micromixer was fabricated incorporating a mixing section comprised of four symmetrically-opposed corner pairs with a pitch of 200 μm , giving an overall length of

Table 1 Mixing indices upstream and downstream of single corner pair

	300 V/cm	350 V/cm	400 V/cm	450 V/cm	500 V/cm
Front of the corners (%)	34.4	33.9	34.4	26.4	26.5
Back of the corners (%)	40.7	39.3	39.1	36.9	32.7

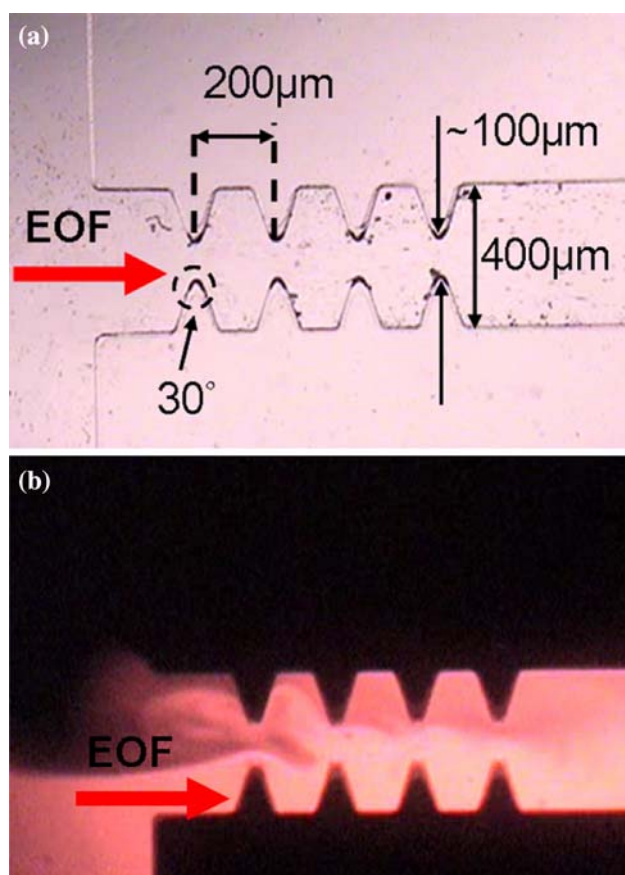


Fig. 6 **a** Flow field structure in serrated mixing region of length 800 μm under external DC electric field with intensity of 210 V/cm. **b** Fluorescent dye (Rhodamine B, 10^{-4} M) observations of species mixing in microchannel with DC electric field intensity of approximately 210 V/cm

approximately 800 μm (see Fig. 6a). As in the case of the single corner pair, each corner had an apex angle of 30° , and the opposing corners in each pair were separated by a distance of approximately 100 μm . During an initial set of experiments, de-ionized water containing latex particles was introduced into the microchannel, and a DC electric field with an intensity of $E \sim 210$ V/cm was applied, prompting the formation of vortex pairs near each set of corner pair (see Fig. 6a). The intensity of the DC electric field was then increased to $E \sim 380$ V/cm.

In the subsequent experiments, Rhodamine B (10^{-4} M) and de-ionized water were introduced into the channel and a DC electric field with an intensity of $E \sim 210$ V/cm was again applied. The resulting flow field structure is shown in Fig. 6b. From inspection, it can be determined that the mixing index increased from 3% in the region of the microchannel upstream of the serrated mixing section to 78% at its outlet. Thus, the experimental results confirm the effectiveness of the vortex structures formed near the individual corners in the serrated mixing section in

enhancing the mixing performance within the microchannel.

4 Concluding remarks

This study presents a special electrokinetic phenomenon that shows vortex generation when wedges were set in a microchannel. The vortex generation in the electroosmotic flow was investigated by a series of experiments. The strength of the induced vortices was affected by the concentration of electrolyte and the intensity of the electric field. The size and strength of the vortex structure increased as the intensity of the DC electric field increased. The reduction in the local concentration of the electrolyte increased the zeta potential in the corner region of the microchannel and, therefore, increased the slip velocity at the microchannel wall. The resulting velocity imbalance between the fluid in the wall region of the microchannel and the bulk flow resulted in the formation of rotating vortices. The experimental results have shown that these vortices created a nozzle-like effect that accelerated the fluid flow in the central region of the microchannel. Furthermore, when two sample streams were introduced simultaneously into the microchannel, the vortices constrained the two samples to the central region of the microchannel and reduced the mixing distance between them, thereby improving their mixing effectiveness. This phenomenon has been exploited in a micromixer, which incorporates a serrated mixing section with a length of 800 μm . The experimental results have revealed that the serrated mixing section yields a mixing index of around 78%, which is a substantial increase over a very short distance. Thus, the utilization of special electrokinetic effects to create a micromixer is possible and confirmed.

Acknowledgments The current authors wish to acknowledge the financial support provided to this study by the National Science Council of Taiwan under Grant No. NSC-96-2628-E-006-162-MY3 and by the National Nano Device Laboratories of Taiwan under Grant No. NDL-95S-C053

References

- Bazant MZ, Squires TM (2004) Induced-charge electrokinetic phenomena: theory and microfluidic applications. *Phys Rev Lett* 92:066101
- Bazant MZ, Thornton K, Ajdari A (2004) Diffuse-charge dynamics in electrochemical systems. *Phys Rev E* 70:021506
- Bazant MZ, Urbanski JP, Levitan JA, Subramanian K, Kilic MS, Jones A, Thorsen T (2007) Electrolyte dependence of AC electro-osmosis. In: *Proceedings of 11th International Conference on Miniaturized Systems for Chemistry and Life Sciences (MicroTAS)*, pp 2875–2878

- Chang CC, Yang RJ (2007) Electrokinetic mixing in microfluidic systems. *Microfluid Nanofluid* 3:501–525
- Chen JK, Yang RJ (2007) Electroosmotic flow mixing in zigzag microchannels. *Electrophoresis* 28:975–983
- Chu KT, Bazant MZ (2006) Nonlinear electrochemical relaxation around conductors. *Phys Rev E* 74:011501
- Cummings EB, Griffiths SK, Nilson RH, Paul PH (2000) Conditions for similitude between the fluid velocity and electric field in electroosmotic flow. *Anal Chem* 72:2526–2532
- Gangwal S, Cayre OJ, Bazant MZ, Velev OD (2008) Induced-charge electrophoresis of metallodielectric particles. *Phys Rev Lett* 100:058302
- Glasgow I, Batton J, Aubry N (2004) Electroosmotic mixing in microchannels. *Lab Chip* 4:558–562
- Hardt S, Drese KS, Hessel V, Schonfeld F (2005) Passive micromixers for applications in the microreactor and μ TAS fields. *Microfluid Nanofluid* 1:108–118
- Johnson TJ, Locascio LE (2002) Characterization and optimization of slanted well designs for microfluidic mixing under electroosmotic flow. *Lab Chip* 2:135–140
- Lazar IM, Karger BL (2002) Multiple open-channel electroosmotic pumping system for microfluidic sample handling. *Anal Chem* 74:6259–6268
- Levitan JA, Devasenathipathy S, Studer V, Ben YX, Thorsen T, Squires TM, Bazant MZ (2005) Experimental observation of induced-charge electro-osmosis around a metal wire in a microchannel. *Colloid Surf A* 267:122–132
- Lin CH, Fu LM, Chien YS (2004) Microfluidic T-form mixer utilizing switching electroosmotic flow. *Anal Chem* 76:5265–5272
- Lin CH, Tsai CH, Fu LM (2005) A rapid three-dimensional vortex micromixer utilizing self-rotation effects under low Reynolds number conditions. *J Micromech Microeng* 15:935–943
- McDonald JC, Whitesides GM (2002) Poly(dimethylsiloxane) as a material for fabricating microfluidic devices. *Acc Chem Res* 35:491–499
- Olesen LH, Bruus H, Ajdari A (2006) AC electrokinetic micropumps: the effect of geometrical confinement, Faradaic current injection, and nonlinear surface capacitance. *Phys Rev E* 73:056313
- Park SY, Russo CJ, Branton D, Stone HA (2006) Eddies in a bottleneck: an arbitrary Debye length theory for capillary electroosmosis. *J Colloid Interface Sci* 297:832–839
- Probstein RF (1994) *Physicochemical hydrodynamics*. Wiley, New York
- Studer V, Pepin A, Chen Y, Ajdari A (2004) An integrated AC electrokinetic pump in a microfluidic loop for fast and tunable flow control. *Analyst* 129:944–949
- Squires TM, Bazant MZ (2004) Induced-charge electro-osmosis. *J Fluid Mech* 509:217–252
- Takhistov P, Duginova K, Chang HC (2003) Electrokinetic mixing vortices due to electrolyte depletion at microchannel junctions. *J Colloid Interface Sci* 263:133–143
- Thamida SK, Chang HC (2002) Nonlinear electrokinetic ejection and entrainment due to polarization at nearly insulated wedges. *Phys Fluids* 14:4315–4328
- Urbanski JP, Thorsen T, Levitan JA, Bazant MZ (2006) Fast AC electro-osmotic micropumps with nonplanar electrodes. *Appl Phys Lett* 89:143598
- Wu J, Ben YX, Chang HC (2005) Particle detection by electrical impedance spectroscopy with asymmetric-polarization AC electroosmotic trapping. *Microfluid Nanofluid* 1:161–167
- Wu CH, Chen JK, Yang RJ (2007) Electrokinetically driven flow control using bare electrodes. *Microfluid Nanofluid* 3:485–494
- Yossifon G, Frankel I, Miloh T (2006) On electro-osmotic flows through microchannel junctions. *Phys Fluids* 18:117108